THE JOURNAL OF PHYSICAL CHEMISTRY A

Article

pubs.acs.org/JPCA

Grid-Based Empirical Improvement of Molecular Potential Energy Surfaces

Tamás Szidarovszky[†] and Attila G. Császár*[,†,‡]

[†]MTA-ELTE Research Group on Complex Chemical Systems, P.O. Box 32, H-1518 Budapest 112, Hungary

[‡]Laboratory on Molecular Structure and Dynamics, Institute of Chemistry, Eötvös University, Pázmány Péter sétány 1/A, H-1117 Budapest, Hungary

ABSTRACT: A grid-based method designed to refine adiabatic potential energy surfaces (PES) of molecules via minimizing a suitable objective function is described. The objective function contains deviations from the reference (experimental) (ro)-vibrational energy levels and is based on PES correction values determined at the grid points within a discrete-variable-representation nuclear-motion algorithm and first-order perturbation theory (PT). The proposed PES refinement technique is tested on the ground electronic state of the MgH molecule. The large number of numerical test results obtained suggest the following: (1) first-order PT is able to yield accurate correction values at the grid points representing the PES, and for practical cases there seems to be no need to go to higher orders of PT; (2) with the number of grid points greatly exceeding the number of experimental energy levels included in the refinement procedure, terms additional to the "obs−calc" term, including numerical first and second derivatives of the correction surface, are necessary in the objective function to arrive at a physically meaningful, "smooth" correction surface; (3) for a given J rotational quantum number, the corrected PES is able to reproduce experimental (ro)vibrational energies to within tenths of cm^{-1} if they are included in the refinement or interpolated between states that are involved in the optimization, whereas extrapolated states tend to have somewhat larger remaining discrepancies; (4) the PES refined only for the $J = 0$ states introduces a minor systematic error for $J > 0$ states, with discrepancies growing with J; (5) when the number of experimental energies included in the refinement greatly exceeds the number of grid points upon which the PES is optimized, the systematic error of treating states with different J rotational quantum numbers can be reduced and an impressive average accuracy can be achieved for all rovibrational states; and (6) in the case of quasibound (also known as resonance) rovibrational states, energies can be computed to accuracies similar to those of the bound states and excellent lifetimes (widths) can also be determined. Changes in thermochemical functions upon inclusion of quasibound states during direct summation is discussed.

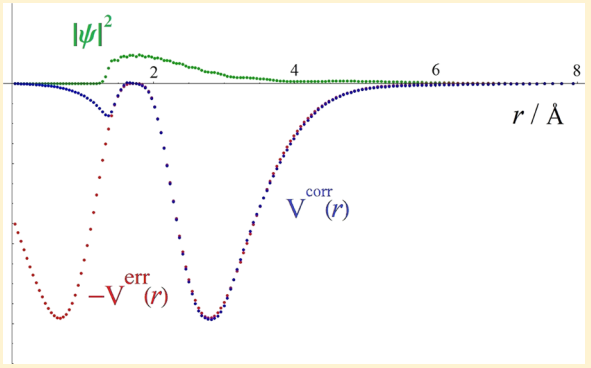

1. INTRODUCTION

Potential energy surfaces (PES), defined within the Born−Oppenheimer approximation,[1] form the basis of most of our chemical concepts. Beyond the qualitative description of chemical phenomena, accurate PESs are used to derive quantitative data employed in diverse fields of chemistry and chemical engineering, including high-resolution molecular spectroscopy (rotational−vibrational energy levels), molecular reaction kinetics and dynamics (reaction rates and lifetimes), and thermochemistry (partition functions and related quantities).

There are several routes that have been explored to produce local or global PES representations; for a couple of possibilities, see refs 2−8. The most common choice to derive a (semi)global PES goes through computing electronic energies *ab initio* at different nuclear coordinate values and fitting them to a suitably chosen functional form. The simplest case for a local representation is to compute energy values and perhaps derivatives, with respect to nuclear coordinates, and to construct a Taylor-series expansion of the PES, yielding an anharmonic force field, preferentially in a set of internal coordinates.[7] Another choice for a local representation is provided by the n-mode incremental scheme of difference potentials (V_i, V_{ij}, etc.) spanned by the normal coordinates q_i of the system.[6] Finally, it is also possible to assume a functional form of the PES with free parameters fitted to experimental data. Often some of the above approaches are mixed; for example, *ab initio* surfaces are corrected using empirical data.[9−11] This is perhaps the most common and at present the most viable way to determine an accurate semiglobal PES for medium-sized many-electron molecules.

In the fourth age of quantum chemistry[12] the extent by which variational nuclear motion computations can be performed requires highly accurate PESs to reproduce experimental

Received: May 3, 2014
Revised: July 11, 2014
Published: July 16, 2014

   dx.doi.org/10.1021/jp504348f | *J. Phys. Chem. A* 2014, 118, 6256−6265

(ro)vibrational spectra within an accuracy of about 0.1 cm^{-1}, which is often needed for the critical validation of related experimental data.[13] Such highly accurate PESs require consideration of relativistic,[14] quantum electrodynamic (QED),[15] and adiabatic corrections,[16] and even a (simplified) treatment of nonadiabatic effects.[17,18] PESs of this quality can only be produced *ab initio* for the simplest few-electron systems.[19] Therefore, a pragmatic way forward for many-electron systems is to develop methods that are capable of improving *ab initio* PESs based on available experimental data. As for the usually studied lighter molecular systems nonadiabatic effects are around 0.1−1 cm^{-1}, and most of the effect can be taken into account by coordinate dependent masses[20−22] or by employing different rotational and vibrational masses,[23] an absolute accuracy greater than about 0.1 cm^{-1} should not be required from an adiabatic PES.

The present paper discusses a deceptively simple approach within grid-based representations of the rovibrational Hamiltonian of nuclear-motion theory, such as the discrete variable representation (DVR),[24−26] for the empirical improvement of PESs: the refinement is achieved by means of minimizing a properly defined objective function measuring basically the difference between experimentally and theoretically obtained eigenenergies of the given system.

2. THEORETICAL FOUNDATIONS

The time-independent nuclear Schrödinger-equation of an M-atomic molecule is

$$\hat{H}\psi^{(i)} = E^{(i)}\psi^{(i)} \tag{1}$$

where $\hat{H} = \hat{T} + \hat{V}$, $\hat{T}$ is the kinetic energy operator expressed in suitable coordinates, $\hat{V}$ is the potential energy operator, and $E^{(i)}$ and $\psi^{(i)}$ are the ith (ro)vibrational energy level and wave function, respectively, corresponding to the given PES depending on $3M - 6$ (geometric) coordinates ($3M - 5$ for linear molecules). Using DVR basis functions and a linear variational approach, the eigenfunctions are approximated by

$$\psi^{(i)} \cong \sum_{l=1}^{N} C_{il}\phi_l^{\mathrm{DVR}} \tag{2}$$

where ϕ_l^{DVR} is the lth DVR basis function, and N is the size of the basis chosen. The matrix representation of eq 1 is

$$\mathbf{H}^{\mathrm{DVR}}\boldsymbol{\psi}^{(i),\mathrm{DVR}} = E^{(i),\mathrm{theory}}\boldsymbol{\psi}^{(i),\mathrm{DVR}} \tag{3}$$

where $\mathbf{H}_{lk} = \langle\phi_l^{\mathrm{DVR}}|\hat{H}|\phi_k^{\mathrm{DVR}}\rangle = \langle\phi_l^{\mathrm{DVR}}|\hat{T}|\phi_k^{\mathrm{DVR}}\rangle + \langle\phi_l^{\mathrm{DVR}}|\hat{V}|\phi_k^{\mathrm{DVR}}\rangle = \mathbf{T}_{lk} + \mathbf{V}_{lk}$, $\boldsymbol{\psi}_l^{(i),\mathrm{DVR}} = C_{il}$, and the matrix elements of the potential energy operator are given by (using the diagonal DVR approximation)

$$\mathbf{V}_{lk} = \langle\phi_l^{\mathrm{DVR}}|\hat{V}|\phi_k^{\mathrm{DVR}}\rangle = V(\mathbf{q}_l^{\mathrm{DVR}})\delta_{lk} \tag{4}$$

where $\mathbf{q}_l^{\mathrm{DVR}}$ is the lth set of quadrature points defined by the DVR basis used; *i.e.*, the potential energy matrix is diagonal, and the diagonal elements are the functional values of the PES at the DVR grid points.

The goal of the PES refinement, the principal topic of this paper, is the determination of a $\Delta V(\mathbf{q})$ "correction surface" represented by the ΔV_l, $l \in \{1, ..., N\}$, correction values yielding a more accurate PES. By defining the correction surface at the grid points, one avoids the problem of making *a priori* assumptions about the form of the correction surface. The grid-based correction surface, determined using perturbation theory preferentially carried out only to first order, improves the $V(\mathbf{q}_l^{\mathrm{DVR}})$ PES values at the DVR grid points in such a way that (a) the refined surface leads to computed $E^{(i),\mathrm{theory}}$ eigenenergies that reproduce some reference (usually experimentally deduced) $E^{(i),\mathrm{exp}}$, $i \in \{1, ..., N^{\mathrm{exp}}\}$, energies as closely as possible (N^{exp} is the number of experimentally available energy values), and (b) the "correction surface" obtained has a physically meaningful and "smooth" form. Requirements (a) and (b) can be formulated mathematically by minimizing a properly defined objective function $F(\Delta V_1,...,\Delta V_N)\} \equiv F(\mathbf{\Delta V})$.

2.1. Objective Functions. If no physical requirements are enforced for the correction surface, and thus the only goal is to reproduce the experimental set of energies used in the refinement procedure, the objective function can be chosen to have the simple form of

$$F^{\mathrm{A}}(\mathbf{\Delta V}) = \sum_{i=1}^{N^{\mathrm{exp}}} (E^{(i),\mathrm{theory,corr}} - E^{(i),\mathrm{exp}})^2 \tag{5}$$

where $E^{(i),\mathrm{theory,corr}}$ are computed energies corresponding to a PES improved by the correction values ΔV_l, $l \in \{1, ..., N\}$. Although the F^{A} objective function might lead to theoretical energies that reproduce the experimental energies with high accuracy, the resulting correction surface might have a physically unsatisfactory form, *i.e.*, have overly large ΔV_l values at certain grid points as well as strong oscillations, which in turn make the corrected PES applicable only for the DVR grid used during the PES optimization, a clearly undesirable property of an empirically corrected PES.

One way to improve the objective function $F^{\mathrm{A}}(\mathbf{\Delta V})$ is to take into account the fact that a physically meaningful correction surface has relatively small values when compared to the original PES obtained *ab initio* or otherwise; thus, overly large correction values during the refinement process should be penalized. The mathematical incorporation of this requirement results in a new objective function,

$$F^{B}(\mathbf{\Delta V}) = \sum_{i=1}^{N^{\mathrm{exp}}} (E^{(i),\mathrm{theory,corr}} - E^{(i),\mathrm{exp}})^2 + \sum_{l=1}^{N} \lambda_l(\Delta V_l)^2 \tag{6}$$

where λ_l are free parameters that need to be set at the beginning of the refinement procedure.

To reduce the undesirable oscillations of the correction surface, $F^{\mathrm{B}}(\mathbf{\Delta V})$ can be extended by terms penalizing ΔV_l corrections that correspond to large first and second derivatives at the grid points, yielding a new objective function

$$F^{C}(\mathbf{\Delta V}) = \sum_{i=1}^{N^{\mathrm{exp}}} (E^{(i),\mathrm{theory,corr}} - E^{(i),\mathrm{exp}})^2 + \sum_{l=1}^{N} \lambda_l(\Delta V_l)^2 + \tilde{\mu} \sum_{l=2}^{N-1} (\Delta V_l')^2 + \tilde{\sigma} \sum_{l=2}^{N-1} (\Delta V_l'')^2 \tag{7}$$

where $\tilde{\mu}$ and $\tilde{\sigma}$ are free parameters set at the beginning of the optimization procedure and $\Delta V_l'$ and $\Delta V_l''$ are numerical approximations of the first and second derivatives of the correction surface at the lth grid point, respectively. Because the grid points used in the nuclear motion computations are not necessarily equidistant, the derivatives should be computed using nonequidistant grid formulas;[27] for example, in this work, the case of a one-dimensional correction surface, the three-point formulas

dx.doi.org/10.1021/jp504348f | J. Phys. Chem. A 2014, 118, 6256−6265

$$\Delta V_l' = \frac{q_{l+1} - q_l}{(q_l - q_{l-1})(q_{l+1} - q_{l-1})}\Delta V_{l-1} + \frac{q_l - q_{l-1}}{(q_{l+1} - q_l)(q_{l+1} - q_{l-1})}\Delta V_{l+1} + \left(\frac{q_{l+1} - q_l}{(q_l - q_{l-1})(q_{l+1} - q_{l-1})} - \frac{q_l - q_{l-1}}{(q_{l+1} - q_l)(q_{l+1} - q_{l-1})}\right)\Delta V_l \quad (8a)$$

and

$$\Delta V_l'' = \frac{2}{(q_l - q_{l-1})(q_{l+1} - q_{l-1})}\Delta V_{l-1} + \frac{2}{(q_{l+1} - q_l)(q_{l+1} - q_{l-1})}\Delta V_{l+1} + \left(-\frac{2}{(q_l - q_{l-1})(q_{l+1} - q_{l-1})} - \frac{2}{(q_{l+1} - q_l)(q_{l+1} - q_{l-1})}\right)\Delta V_l \quad (8b)$$

were employed.

2.2. Evaluation of Objective Functions. On the basis of the assumption that the correction surface is small when compared to the original PES, the effect of $\Delta V(\mathbf{q})$ on the theoretical energies can be taken into account via first-order perturbation theory (PT1); *i.e.*, correction energies with a given set of ΔV_l values are computed as

$$\begin{aligned} E^{(i),\mathrm{theory,corr}} &= E^{(i),\mathrm{theory}} + \langle \psi^{(i)} | \Delta V \psi^{(i)} \rangle \\ &= E^{(i),\mathrm{theory}} + \sum_{l,k=1}^{N} C_{il}^* C_{ik} \langle \varphi_l^{\mathrm{DVR}} | \Delta V \varphi_k^{\mathrm{DVR}} \rangle \\ &= E^{(i),\mathrm{theory}} + \sum_{l,k=1}^{N} C_{il}^* C_{ik} \Delta V(\mathbf{q}_l^{\mathrm{DVR}}) \delta_{lk} \\ &= E^{(i),\mathrm{theory}} + \sum_{k=1}^{N} |C_{ik}|^2 \Delta V_k \end{aligned} \quad (9)$$

Here the considerable advantage of the proposed correction built upon a grid-based representation of the Hamiltonian and PT1 can be seen vividly as determination of the correction energies requires a minimum amount of computational effort.

The effect of second-order perturbation theory (PT2) terms for computing the correction energies will be discussed in section 4.

2.3. Minimizing the Objective Function. Whichever objective function, F^{A}, F^{B}, or F^{C}, is chosen, its minimum can be obtained by standard numerical approaches.[28] For the above perturbative case the minimization can be reduced to solving a system of inhomogeneous linear equations of size $N \times N$. This is easily manageable for diatomic molecules, where the DVR grid size is on the order of a hundred points. Using $F^{\mathrm{C}}(\mathbf{\Delta V})$, for example, the requirements for the minimum are $\partial_{\Delta V_l} F^{\mathrm{C}}(\mathbf{\Delta V}) = 0$, which leads to the system of linear equations

$$(\mathbf{A}^{(1)} + \mathbf{A}^{(2)} + \mathbf{A}^{(3)} + \mathbf{A}^{(4)})\mathbf{\Delta V} = \mathbf{b} \quad (10)$$

where $\mathbf{\Delta V}, \mathbf{b} \in \mathbb{R}^N$ $\mathbf{A}^{(1)}, \mathbf{A}^{(2)}, \mathbf{A}^{(3)}, \mathbf{A}^{(4)} \in \mathbb{R}^{N\times N}$ with $(\mathbf{\Delta V})_l = \Delta V_l$,

$$b_l = \sum_{i=1}^{N^{\mathrm{exp}}} (E^{(i),\mathrm{exp}} - E^{(i),\mathrm{theory}})|C_{il}|^2$$

$$A_{lk}^{(1)} = \sum_{i=1}^{N^{\mathrm{exp}}} |C_{il}|^2 |C_{ik}|^2 \qquad A_{lk}^{(2)} = \lambda_l \delta_{lk}$$

$$A_{lk}^{(3)} = \frac{\mu}{\mathrm{Mean}[\{a_i^{(3)}\}_{i=2}^{n-1}]}[a_{l-1}^{(3)} c_{l-1}^{(3)} \delta_{kl-2} + (a_l^{(3)} b_l^{(3)} + b_{l-1}^{(3)} c_{l-1}^{(3)})\delta_{kl-1} + (a_l^{(3)} a_l^{(3)} + b_l^{(3)} b_l^{(3)} + c_l^{(3)} c_l^{(3)})\delta_{kl} + (a_{l+1}^{(3)} b_{l+1}^{(3)} + b_l^{(3)} c_l^{(3)})\delta_{kl+1} + a_{l+1}^{(3)} c_{l+1}^{(3)} \delta_{kl+2}]$$

$$A_{lk}^{(4)} = \frac{\sigma}{\mathrm{Mean}[\{a_i^{(4)}\}_{i=2}^{n-1}]}[a_{l-1}^{(4)} c_{l-1}^{(4)} \delta_{kl-2} + + (a_l^{(4)} b_l^{(4)} + b_{l-1}^{(4)} c_{l-1}^{(4)})\delta_{kl-1} + (a_l^{(4)} a_l^{(4)} + b_l^{(4)} b_l^{(4)} + c_l^{(4)} c_l^{(4)})\delta_{kl} + (a_{l+1}^{(4)} b_{l+1}^{(4)} + b_l^{(4)} c_l^{(4)})\delta_{kl+1} + a_{l+1}^{(4)} c_{l+1}^{(4)} \delta_{kl+2}]$$

$$a_l^{(3)} = -\frac{q_{l+1} - q_l}{(q_l - q_{l-1})(q_{l+1} - q_{l-1})} \qquad b_l^{(3)} = -a_l^{(3)} - c_l^{(3)}$$

$$c_l^{(3)} = \frac{q_l - q_{l-1}}{(q_{l+1} - q_l)(q_{l+1} - q_{l-1})}$$

$$a_l^{(4)} = \frac{2}{(q_l - q_{l-1})(q_{l+1} - q_{l-1})} \qquad b_l^{(4)} = -a_l^{(4)} - c_l^{(4)}$$

$$c_l^{(4)} = \frac{2}{(q_{l+1} - q_l)(q_{l+1} - q_{l-1})}$$

and

$$\mu = \tilde{\mu} \cdot \mathrm{Mean}[\{a_i^{(3)}\}_{i=2}^{n-1}] \quad \text{and} \quad \sigma = \tilde{\sigma} \cdot \mathrm{Mean}[\{a_i^{(4)}\}_{i=2}^{n-1}]$$

By solving eq 10, we arrive at optimal ΔV_l values (within PT1, corresponding to a given objective function as well as given λ_l, μ, and σ parameters) that can be fitted with a functional form or a spline, to obtain $\Delta V(\mathbf{q})$.

After a set of correction values on the DVR grid, or the related correction surface, is obtained, the optimization procedure might be repeated again and again, using the previously corrected surface as the initial one. This iterative approach is most useful when the starting PES is too far from the "ideal PES", as in this case the above-described PT approach does not yield satisfactory correction results in a single step.

3. COMPUTATIONAL DETAILS

The test system chosen for this study is the MgH molecule in its ground electronic state. There are experimental data available on bound and also on quasibound (resonance) (ro)vibrational states of MgH,[29] along with a highly accurate PES function, called MLR and obtained by Le Roy et al.,[7] which can be used as a reference PES to measure the quality of approximate surfaces. The theoretical rovibrational states of MgH obtained with the MLR PES reproduce experimental transition energies with an accuracy of a few tenths of cm^{-1} when a Born−Oppenheimer breakdown function and spin-rotation interaction corrections are included (see ref 7). In our empirical refinement procedure the adiabatic energies obtained with the MLR PES were used as the reference "experimental" energies.

dx.doi.org/10.1021/jp504348f | J. Phys. Chem. A 2014, 118, 6256−6265

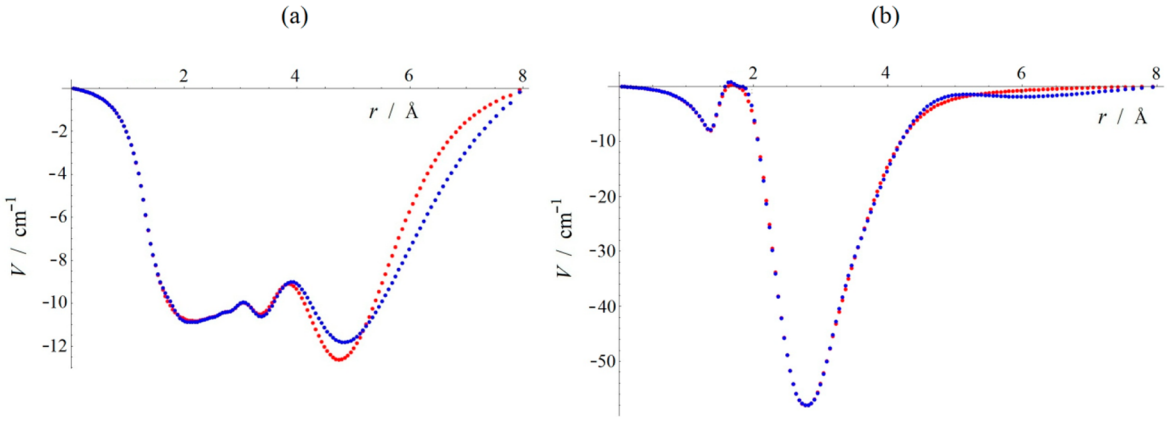

Figure 1. Pictorial representation of the optimized PES correction values obtained using PT1 (red dots) or PT2 (blue dots) when evaluating the effect of correction energies on the purely vibrational energy values. All 12 $J = 0$ eigenstates were included in the objective function F^C. (a) The correction values obtained for $V_1^{DS}(r)$ correspond to $\lambda_l = 0.0001$, $\mu = 0.001$, and $\sigma = 0.001$. (b) The correction values obtained for $V_2^{DS}(r)$ correspond to $\lambda_l = 0.001$, $\mu = 0.01$, and $\sigma = 0.01$.

The initial PESs, those to be corrected, are generated by adding "discrepancy surfaces" to the MLR PES. From the many surfaces tested, two functional forms are reported herein, a constant discrepancy surface $V_1^{DS}(r) = 10$ cm^{-1}, and another one, $V_2^{DS}(r) = 200(r - r_e)^4 e^{-2|r-r_e|}$ cm^{-1}, where $r_e = 3.26863$ bohr. $V_1^{DS}(r)$ was chosen to provide visually simplified information on the properties of the PES refinement procedure. $V_2^{DS}(r)$ was chosen to represent a realistic "discrepancy surface", as $V_2^{DS}(r)$ is small near the minimum of the PES and near dissociation, whereas it has a maximum at an intermediate distance. Because the $V_2^{DS}(r)$ surface has values of several tens of cm^{-1}, the minimization of the objective function had to be iteratively repeated. The final optimized correction surface was represented by spline interpolation with the help of the determined correction values at the grid points.

(Ro)vibrational eigenenergies used during the PES optimizations were obtained by solving the diatomic (ro)vibrational time-independent Schrödinger-equation using 150 spherical-oscillator-DVR[30] basis functions. The DVR quadrature points lie between internuclear distances of 0.0802 and 15 bohr. For testing the accuracy of a refined PES, 140 spherical-oscillator-DVR basis functions were used, with DVR points lying between 0.0832 and 14.5 bohr. The latter was done to have test results with DVR grid points different from the ones used during the optimization. The eigenenergies of all variational-type rovibrational computations are converged to better than 0.1 cm^{-1}.

Computation of the quasibound states (having exponentially divergent wave functions, see section 4.4) requires using the methods of non-Hermitian quantum chemistry.[31] A complex absorbing potential (CAP) of the form

$$V_{CAP}(r) = -i\eta W(r)$$

was used, where

$$W(r) = \begin{cases} 0, \text{ if } r < r_{min} \\ 2.1758\dfrac{r - r_{min}}{r_{max} - r_{min}} + 3.3108\left(\dfrac{r - r_{min}}{r_{max} - r_{min}}\right)^3 \\ \quad + 4.3226\left(\dfrac{r - r_{min}}{r_{max} - r_{min}}\right)^5, \text{ if } r \geq r_{min} \end{cases}$$

was taken from ref 32, with parameters $r_{min} = 10.0$ bohr and $r_{max} = 14.5$ bohr, and the optimal η (CAP strength parameter) was determined for each quasibound state separately by identifying cusps in the complex eigenvalue trajectories.[33]

4. RESULTS AND DISCUSSION

Various objective functions were tested during the empirical refinement of the initial MgH PESs, involving different sets of experimental data and optimization of the many parameters mentioned in section 2.1. As the results obtained with the objective function $F^C(\mathbf{\Delta V})$ appear to be the most useful, these are discussed in detail below. To test the effect of including second-order PT terms into the objective function during the determination of correction energies, correction surfaces were computed using either PT1 or PT2 terms in the objective function $F^C(\mathbf{\Delta V})$ starting from initial PESs obtained with $V_1^{DS}(r)$ and $V_2^{DS}(r)$. As presented in Figure 1, the correction surfaces for PT1 and PT2 are almost identical up to an internuclear distance of 4 Å, beyond which correction value differences can reach 1−2 cm^{-1}. Because beyond an internuclear distance of 4 Å only a minor part of the highest-energy $v = 11$ vibrational state wave function has significant amplitude and solving the nonlinear equations (the analog of eq 10) for PT2 is much more expensive than eq 10 for PT1, only the latter was used in the subsequent calculations. The shape of the correction surface corresponding to $V_1^{DS}(r)$ requires a brief discussion. The presence of only two states with significant amplitude above 3 Å is the reason for the oscillations in the correction surfaces in Figure 1a. Note that the effect of a given grid point in the objective function is weighted by the wave function amplitudes at that point; therefore, the presence of one (or two) "significant" wave function means that the correction surface will inherit the structure of that wave function. In the following, only the initial PES with the $V_2^{DS}(r)$ surface is considered.

4.1. $J = 0$ States. The MLR PES of MgH supports 12 bound vibrational states. The number of DVR grid points is 150; thus, there are many more parameters than input data. If one uses the objective function $F^C(\mathbf{\Delta V})$ with very small or zero μ and σ values, the experimental energy values can be reproduced to arbitrary accuracy. However, the correction values obtained this way represent a nonphysical correction surface with large oscillations (Figure 2a). Therefore, one should use an objective function which decreases the number of free parameters by choosing appropriate μ and σ values, *i.e.*,

dx.doi.org/10.1021/jp504348f | J. Phys. Chem. A 2014, 118, 6256−6265

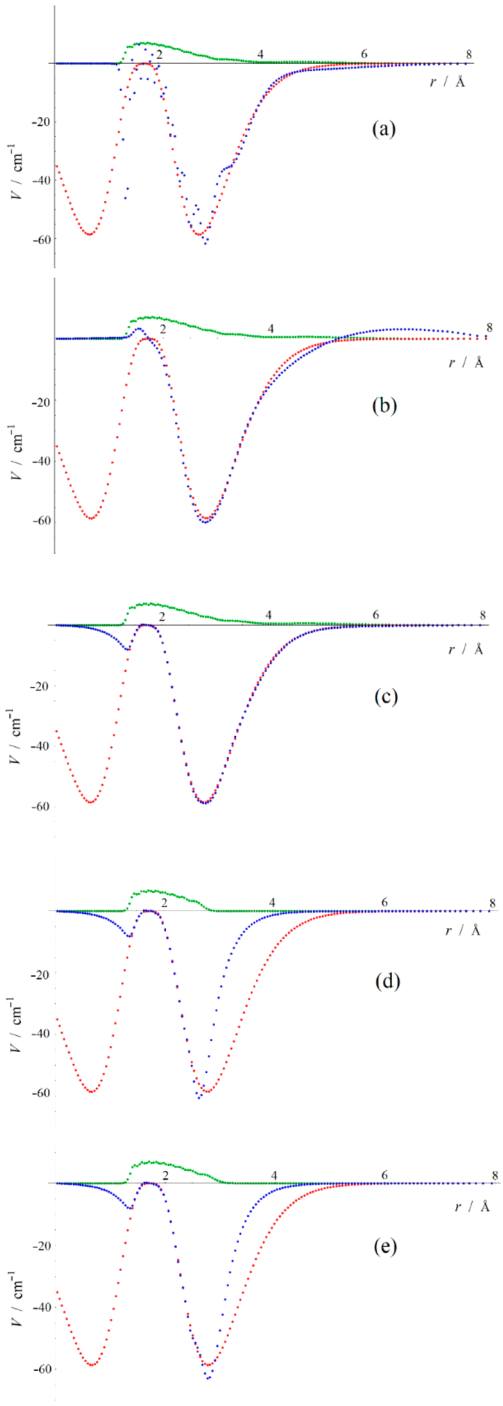

Figure 2. Pictorial representation of the $-V_2^{DS}(r)$ function (red dots), the optimized PES correction values (blue dots), and the sum of the probability density of states included in the optimization (green dots): (a) $v = 0-11$ states included with $\lambda_l = 0.001$, $\mu = 0.00001$, and $\sigma = 0.00001$; (b) $v = 0-11$ states included with $\lambda_l = 0.00001$, $\mu = 0.01$, and $\sigma = 0.01$; (c) $v = 0-11$ states included with $\lambda_l = 0.001$, $\mu = 0.01$, and $\sigma = 0.01$; (d) $v = 0-5$ states included with $\lambda_l = 0.01$, $\mu = 0.1$, and $\sigma = 0.1$; (e) $v = 0-8$ states included with $\lambda_l = 0.0005$, $\mu = 0.005$, and $\sigma = 0.005$.

requiring "smoothness" from the correction surface. However, the optimal choice for μ and σ is not straightforward. If these parameters are too large, the empirical refinement procedure might lead to correction surfaces that are "forced" into a nonphysical form by the terms containing the numerical derivatives in the objective function. An example can be seen in Figure 2b, where the sign change of the correction surface at around 5.2 Å and its slow damping to zero near dissociation is clearly a sign of "rigidity" introduced by too large μ and σ values with respect to λ_l. Our extensive numerical testing suggests that the optimal μ and σ can be found by starting out with very small values (with respect to the λ_l values, which should be chosen to ensure the damping of the correction surface to zero at coordinate regions where the wave functions included in the optimization do not have significant amplitudes) and gradually increasing them up to the point where the correction surface becomes "smooth" enough; *i.e.*, oscillations on neighboring grid points become smaller than a few tenths of cm^{-1}. The λ_l parameters usually turned out to be an order of magnitude smaller than μ and σ.

"Smoothness" of the correction surface could be tested by visual inspection; however, this might be difficult to extend to polyatomic molecules with multidimensional PESs. Therefore, a properly defined quantity for measuring the "smoothness" of the correction surface would seem to be useful. We found that for this purpose the

$$S(\lambda_1,...,\lambda_N,\mu,\sigma) = |\Delta\mathbf{V} - \Delta\mathbf{V}^{\text{Smoothed}}|/N \quad (11)$$

norm appears to be appropriate, where $\Delta\mathbf{V}^{\text{Smoothed}}$ is obtained from $\Delta\mathbf{V}$ by taking its discrete convolution with a smoothing kernel $\mathbf{K}$. In this work the kernels $\mathbf{K}^{(1)} = (1, 2, 1)/4$ and $\mathbf{K}^{(2)} = (1, 1, 2, 1, 1)/6$ were used, hence $\Delta V_l^{\text{Smoothed}} = \sum_k \Delta V_{l-k} K_k^{(i)}$ with $k \in \{-1, 0, 1\}$for $i = 1$ and $k \in \{-2, -1, 0, 1, 2\}$ for $i = 2$. Figure 3 presents the norm in eq 11 obtained with different parameter values and the two kernels. As clear from the figure, the two smoothing kernels show essentially the same behavior: for very small (effectively zero) μ values S is more or less constant, whereas increasing μ leads to a steep drop in S as the effect of the numerical derivatives "kicks in" and the correction surface starts to become smoother. By a further increase in μ, S reaches a slowly changing domain, which corresponds to the correction surface being already "smooth" and becoming more and more "rigid". Our suggestion for the optimal value of μ is the part where S reaches the lower "plateau". The visual inspection of the correction surface for determining the optimal μ value suggested $\mu = 0.01$ (Figure 2c), which is in agreement with Figure 3. Unlike the visual inspection technique, constructing S for multidimensional surfaces is straightforward by using multidimensional smoothing kernels.

Table 1 summarizes energies obtained with optimized PESs determined by including different number of experimental vibrational levels in the objective function (the iteration procedure was terminated when the largest correction value between two consecutive cycles decreased below 0.1 cm^{-1}). Pictorial representation of the optimized PES corrections can be seen in Figure 2c–e. As clear from Table 1, the optimized PES improves the accuracy of the vibrational eigenvalues considerably for states included in the objective function, and works almost as well for states lying between states that are included in the objective function. Regarding the latter case, one can see in the last two columns of Table 1 that omitting the $v = 4$ state has no visible effect on the energies obtained with the optimized PES, whereas omitting the $v = 7$ state does lead to a small error. This could be explained by the fact that the $v = 4$ wave function has relevant amplitudes at coordinate ranges where other wave functions also contribute significantly, whereas this holds less for the $v = 7$ state. As expected, energies lying "outside" the energy range of the states included in the optimization are much less accurate than the ones

dx.doi.org/10.1021/jp504348f | J. Phys. Chem. A 2014, 118, 6256–6265

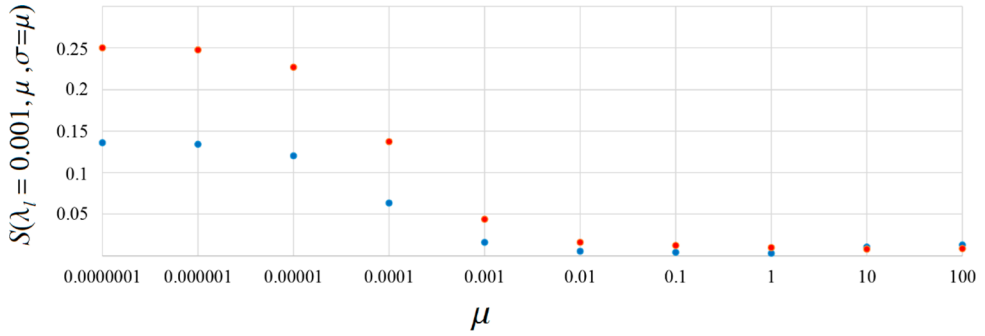

Figure 3. Pictorial representation of $S(\lambda_1,...,\lambda_N,\mu,\sigma)$ from eq 11 as a function of μ, using the smoothing kernel $\mathbf{K}^{(1)}$ (blue dots) or $\mathbf{K}^{(2)}$ (red dots), with $\lambda_l = 0.001$ and $\sigma = \mu$.

Table 1. "Experimental" Vibrational ($J = 0$) Energies of MgH along with Discrepancies of the Theoretical Values Corresponding to Refined PESs Obtained by Considering Different Number of Vibrational States in the Objective Function (All Energies in cm^{-1})

v	expt[a]	no opt[b]	0−11[c,d]	0−8[c,e]	0−5[c,f]	0−3 and 5−11[c,g]	0−6 and 8−11[c,g]
0	0.00	0.52	0.00	0.00	−0.02	0.00	0.00
1	1431.98	2.58	−0.01	0.00	0.00	−0.01	−0.01
2	2800.68	6.21	0.00	0.00	0.11	0.00	0.00
3	4102.33	10.85	0.00	0.00	0.01	0.00	0.00
4	5331.39	16.17	0.00	0.00	−0.42	0.00	0.01
5	6479.66	21.88	0.00	−0.01	0.33	0.00	−0.03
6	7534.81	27.80	0.00	0.03	5.60	0.00	0.02
7	8478.00	33.61	0.01	−0.03	13.18	0.01	0.39
8	9279.65	38.69	−0.01	0.01	21.46	−0.01	−0.01
9	9892.72	40.57	0.01	6.73	28.24	0.01	0.00
10	10249.41	28.24	0.00	12.85	23.37	0.00	0.00
11	10353.25	5.33	0.10	3.20	4.76	0.10	0.10

[a]Obtained with the MLR PES of ref 7. The D_0 dissociation energy is 10 365.1 cm^{-1}. [b]Obtained with the initial PES. [c]The numbers represent the v values of the vibrational states included during the optimization. [d]The free parameters during the refinement were chosen to be $\lambda_l = 0.001$, $\mu = 0.01$, and $\sigma = 0.01$. [e]The free parameters during the refinement were chosen to be $\lambda_l = 0.0005$, $\mu = 0.005$, and $\sigma = 0.005$. [f]The free parameters during the refinement were chosen to be $\lambda_l = 0.01$, $\mu = 0.1$, and $\sigma = 0.1$. [g]The free parameters during the refinement were chosen to be $\lambda_l = 0.001$, $\mu = 0.01$, and $\sigma = 0.01$.

"inside" the energy range, as states with increasing energy have significant amplitudes at larger coordinate ranges; thus, optimizing the PES for lower-energy states has less effect on the grid points that are important for the higher-energy states.

4.2. $J = 10$ States. Table 2 presents $J = 0$ vibrational and $J = 10$ rovibrational energies computed with the initial PES, the PES optimized with $J = 0$ vibrational states, and the PES optimized with $J = 10$ states. The PES refined using only vibrational states results in a more or less systematic and very small error for the rovibrational states, and vice versa, except for the $J = 0$ states with $v = 10$ and $v = 11$, which have larger error. This is expected, however, as these states do not exist for $J = 10$ and thus are omitted during the $J = 10$ optimization.

4.3. All J. During all optimizations in the previous sections the number of DVR grid points, 150, was much larger than the number of experimental eigenenergies, 5−12, included in the objective function. However, if one includes all the 318 bound (ro)vibrational states of MgH (up to $J = 44$, supported by the MLR PES) in the optimization procedure, the situation becomes just the opposite. The last column of Table 2 presents the error of theoretical energies for $J = 0$ and $J = 10$ for the case where all bound (ro)vibrational states (up to $J = 44$) are used in the optimization. Both the $J = 0$ and $J = 10$ results have remarkable accuracy and are just slightly less accurate than the ones obtained by optimizing only for the given J values. Table 3 demonstrates average absolute theoretical energy discrepancies, with respect to the experimental energies, in the case when all bound (ro)vibrational states (up to $J = 44$) are used during the refinement of the PES. Averaging was carried out for fixed v and J values. For all vibrational and rotational quantum numbers an excellent average accuracy, of a few hundredths cm^{-1}, could be achieved. It is noted that the convergence of the iterative optimization procedure was somewhat slower than during the optimization for a given J value and the refinement was stopped when all correction values became smaller than 0.2 cm^{-1}.

4.4. Quasibound States. Resonance states (also known as quasibound or metastable states) of molecular systems have sufficient energy to break up the system into subsystems.[34,35] They are associated with wave functions having outgoing boundary conditions and are characterized by complex eigenvalues usually written as $E_n^{res} = \varepsilon_n - (i/2)\Gamma_n$, where $\varepsilon_n = \mathrm{Re}(E_n^{res})$ is the resonance energy and Γ_n is the width of the resonance state, related to the inverse lifetime at a given $\mathbf{q}$ point in coordinate space by $\rho_n(\mathbf{q},t) \propto e^{-\Gamma_n t}$ (in atomic units), where $\rho_n(\mathbf{q},t) = |\psi_n^{res}|^2$ and ψ_n^{res} is the nth resonance wave function. For rotationally excited diatomic molecules, resonance states can be formed by the molecule trapped behind a centrifugal barrier with energy higher than required for dissociation. In such cases breaking of the molecule occurs via tunneling through the

dx.doi.org/10.1021/jp504348f | J. Phys. Chem. A 2014, 118, 6256−6265

Table 2. $J = 0$ "Experimental" Vibrational ("expt") and $J = 10$ Rovibrational Energies of MgH and the Deviations of the Theoretical Values Corresponding to Optimized PESs Obtained by Including Different Number of (Ro)Vibrational States into the Objective Function (All Energies in cm^{-1})

v	expt[a]	no opt[b]	0−11 vib[c,d]	0−10 rovib[c,d]	all rovib[e]
			$J = 0$		
0	0.00	0.52	0.00	0.01	0.00
1	1431.98	2.58	−0.01	−0.02	0.00
2	2800.68	6.21	0.00	0.00	0.00
3	4102.33	10.85	0.00	0.03	0.00
4	5331.39	16.17	0.00	0.05	0.01
5	6479.66	21.88	0.00	0.06	0.00
6	7534.81	27.80	0.00	0.10	0.03
7	8478.00	33.61	0.01	0.09	0.07
8	9279.65	38.69	−0.01	0.15	0.08
9	9892.72	40.57	0.01	−0.27	0.01
10	10249.41	28.24	0.00	3.07	0.07
11	10352.25	5.33	0.10	1.82	0.09
			$J = 10$		
0	626.74	0.58	−0.02	0.00	0.00
1	2038.77	2.85	−0.01	0.00	0.00
2	3386.76	6.71	−0.01	0.00	0.00
3	4666.54	11.57	−0.04	0.00	0.00
4	5871.93	17.08	−0.07	0.00	0.01
5	6993.74	22.97	−0.09	0.00	0.01
6	8017.96	29.01	−0.13	0.00	0.00
7	8922.68	34.91	−0.15	0.00	0.01
8	9672.38	39.75	−0.20	0.00	0.02
9	10206.59	39.18	−0.02	0.00	0.01

[a]Obtained with the MLR PES of ref 7. The D_0 dissociation energy is 10 365.1 cm^{-1}. [b]Obtained by applying the $V_2^{DS}(r)$ discrepancy surface to the MLR PES. [c]These numbers represent the v values of the(ro)vibrational states included during the optimization. [d]Parameters during the optimization were $\lambda_l = 0.001$, $\mu = 0.01$, and $\sigma = 0.01$. [e]PES optimized with all (ro)vibrational states up to $J = 44$ with parameters $\lambda_l = 0.01$, $\mu = 0.03$, and $\sigma = 0.03$.

Table 3. Averages of the Absolute Values of Theoretical Energy Discrepancies (with Respect to the "Experimental" Energies Obtained with the MLR PES of Ref 7), Computed Using the Initial PES ("no opt") and the PES Optimized by Including All Bound (Ro)Vibrational States (up to $J = 44$) in the Objective Function ("all rovib")[a]

v	no opt	all rovib[b]	J	no opt	all rovib[b]	J	no opt	all rovib[b]
0	1.77	0.03	0	19.36	0.03	22	15.81	0.01
1	5.26	0.02	1	19.33	0.03	23	16.19	0.01
2	9.60	0.01	2	19.29	0.03	24	16.59	0.01
3	14.55	0.01	3	19.21	0.04	25	17.01	0.01
4	19.63	0.02	4	20.54	0.02	26	14.28	0.00
5	25.14	0.01	5	20.46	0.02	27	14.72	0.00
6	30.45	0.01	6	20.34	0.02	28	15.18	0.00
7	35.54	0.00	7	20.15	0.02	29	15.69	0.00
8	39.63	0.00	8	20.29	0.01	30	12.87	0.00
9	39.87	0.00	9	20.37	0.01	31	13.38	0.00
10	25.40	0.00	10	20.46	0.01	32	13.91	0.00
11	4.70	0.00	11	20.54	0.01	33	11.06	0.00
			12	20.61	0.01	34	11.59	0.00
			13	18.91	0.01	35	12.16	0.00
			14	19.12	0.01	36	12.77	0.00
			15	19.34	0.02	37	9.82	0.00
			16	19.57	0.02	38	10.41	0.00
			17	19.81	0.02	39	11.04	0.00
			18	17.46	0.01	40	7.98	0.00
			19	17.76	0.01	41	8.58	0.00
			20	18.09	0.02	42	9.23	0.00
			21	18.43	0.02	43	5.97	0.00
						44	6.57	0.00

[a]Averaging was carried out for fixed v and J values. All energies are given in cm^{-1}. [b]PES optimized with all (ro)vibrational states up to $J = 44$ with parameters $\lambda_l = 0.01$, $\mu = 0.03$, and $\sigma = 0.03$.

centrifugal barrier, which gives rise to the exponential decay in time.

Table 4 presents resonance energies and widths, either measured or computed using the MLR and the refined PESs. As seen in Table 4, with the initial "distorted" PES resonance energies have quite large errors; *i.e.*, for $v = 4$−7 the errors are larger than the average errors for the corresponding bound states (cf. column 2 of Table 3). Both refined PESs redeem this problem, they reproduce the MLR results to a higher accuracy than the discrepancy of the adiabatic MLR results with respect to measured values. Similarly to bound states, inclusion of a large number of rovibrational states in the optimization procedure, additionally to the vibrational states, leads to more accurate results; *i.e.*, the resonance energies and widths under "all rovib" reproduce the values of the "MLR" columns better than the numbers given in the "0−11 vib" columns.

As a next step, one might ask whether including resonance states into the objective function during the optimization procedure would lead to a more accurate refined PES. Figure 4a shows the $J = 0$ vibrational, the $J = 32$ bound rovibrational, and the $J = 39$ quasibound rovibrational probability density functions for $v = 4$. As the figures suggest, with increasing J the wave functions are shifted to larger internuclear distances; therefore, for a given v inclusion of resonance states into the objective function should result in significant wave function amplitudes at coordinate values where bound states vanish. This fact suggests that the inclusion of resonance states into the objective function not only improves the "number of states included/optimized parameters" ratio but also extends the coordinate range having significant wave function amplitude. This is only true, however, if bound states corresponding to other v vibrational quantum numbers included in the objective function do not have significant amplitudes at the coordinate values where the resonance wavefuntions are located. Panels b and c of Figure 4 both show the total probability density for the resonance states included in Table 4 along with the total probability density for all the bound states (up to $J = 44$) supported by the MLR PES. It is clearly seen in Figure 4b,c that, at least for MgH, including the resonance states of Table 4 into the objective function does not introduce significant wave function amplitude at coordinate ranges where bound states vanish, it only improves the "number of states included/optimized parameters" ratio.

4.5. A Detour to Thermochemistry. Although seldom considered, resonance states can play an important role in thermochemistry at elevated temperatures. To illustrate this point, all the 638 bound rovibrational states of MgH supported by the MLR PES (up to $J = 44$, including electronic spin-rotation and nonadiabatic corrections) and an additional 388 resonance states (up to $J = 66$ and below 20 000 cm^{-1} above the ZPVE) were used to construct the canonical partition function

dx.doi.org/10.1021/jp504348f | J. Phys. Chem. A 2014, 118, 6256−6265

Table 4. Rovibrational Resonance Energies, Relative to the Dissociation Threshold, and Widths of MgH Obtained from Experiment or Computed Using the MLR PES of Ref 7 and Two PESs Refined within This Work, One Based on All Bound Vibrational States (J = 0) and the Other on All Rovibrational States (up to J = 44)[a]

		expt[b]		MLR[c]		no opt[e]		0−11 vib[d,e]		all rovib[d,e]	
v	J	ε	Γ	ε	Γ	$\Delta\varepsilon$	$\Delta\Gamma$	$\Delta\varepsilon$	$\Delta\Gamma$	$\Delta\varepsilon$	$\Delta\Gamma$
4	39			1698.8	0.02	35.4	0.00	−0.4	0.00	0.0	0.00
4	40	1978.4	0.47	1977.2	0.65	36.9	−0.25	−0.4	0.00	0.0	0.00
5	35	1322.6	0.11	1321.6	0.11	38.5	0.03	−0.4	0.00	−0.1	0.00
6	30			830.4	0.04	40.0	0.03	−0.4	0.00	−0.1	0.00
6	31	1028.1	1.05	1027.3	0.94	41.1	0.10	−0.3	−0.01	0.0	0.00
7	25			491.2	0.05	41.0	0.20	−0.3	0.00	−0.1	0.00
7	26	645.3	1.15	644.2	1.75	41.6	0.25	−0.1	0.00	0.0	0.01
8	20	279.5	0.16	279.5	0.15	39.4	0.85	−0.2	0.00	−0.1	0.00
9	14	88.5	0.05	88.8	0.07	32.9	1.15	0.1	0.00	0.1	0.00

[a]Note that experiment (expt) here refers to true measured results, as opposed to the previous tables, where it referred to the MLR results. [b]Experimental values are taken from Table 2 of ref 29. [c]Computations were carried out using the MLR PES of ref 7. [d]See footnote c to Table 2. [e]The values are relative to the MLR results.

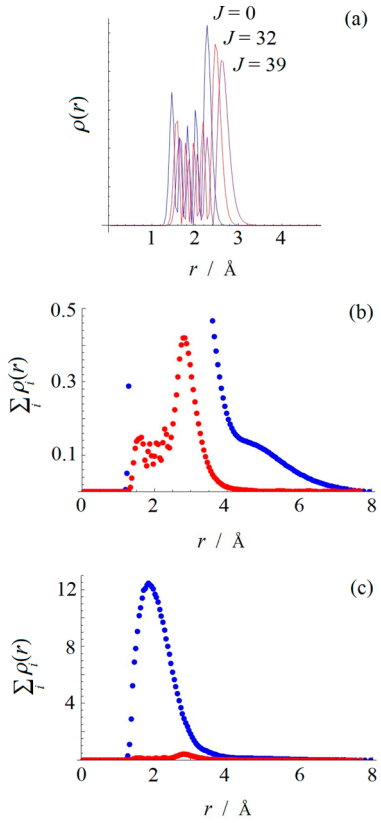

Figure 4. Pictorial representation of (a) v = 4 probability density functions for the J = 0 vibrational, J = 32 bound rovibrational, and J = 39 quasibound rovibrational states, and (b, c) total probability density functions for all the bound (up to J = 44) states (blue dots) along with total probability density functions for all resonance states included in Table 4 (red dots).

$$Q(T) = \int_0^\infty \rho(E) e^{-\beta E}\, dE = \sum_n g_n e^{-\beta E_n} + \frac{1}{2\pi}\sum_r g_r \int_{D_e}^\infty \frac{\Gamma_r e^{-\beta E}}{(E-\varepsilon_r)^2 + \Gamma_r^2/4}\, dE \quad (12)$$

where $\rho(E)$ is the density of states, $\beta = 1/kT$, k is Boltzmann's constant, T is the thermodynamic temperature, g_i stands for the overall degeneracy of state i, and the summation over n and r goes over bound states and resonance states, respectively.[36,37] From $Q(T)$ the C_p heat capacity at different temperatures can be calculated. The effect of resonance states can be monitored by repeating the partition function calculation of each $C_p(T)$ value with and without the resonance states. At 300 K no effect of the quasibound states is observed, but at 1500, 3000, and 4000 K the inclusion of resonance states into the partition function leads to a 0.9, 14.7, and 19.5% increase in the heat capacity, respectively.

4.6. Extension to Polyatomic Molecules. Application of the PES refinement technique presented to polyatomic molecules, although straightforward in principle, may need special considerations: (1) As the dimension of the DVR grid increases, the objective function might need to contain more terms, as the number of partial first and second derivatives also increases. (2) For a triatomic molecule, the number of DVR grid points may be hundreds of thousands, and for molecules with four or more atoms this can reach the millions. Therefore, solving eq 10 is not possible if one takes into account all the grid points. However, the majority of the grid points might be omitted during the optimization if the wave functions do not have significant amplitudes there; thus, the optimization could be carried out for a reduced set of grid points and the correction surface extended to the whole set of grid points subsequently. Nonetheless, even if eq 10 is not solvable, the minimum of the objective function used might be found by using a gradient method from a "good" starting vector $\Delta V_l = 0$, l = 1, ..., N. (3) A selection procedure among grid points can be implemented reducing the number of points considered and perhaps interpolating on the basis of the improved potential information. (4) When one optimizes the parameters in the objective function, visual inspection of the "smoothness" of the correction surface for polyatomic cases is more difficult than in the diatomic case, as one might need to examine several cuts of the surface. Nonetheless, evaluation of the "smoothness" norm in eq 11 is straightforward to extend to higher dimensional surfaces by using an appropriate dimensional smoothing kernel for the convolution with $\Delta\mathbf{V}$.

5. SUMMARY AND CONCLUSIONS

This study demonstrates the usefulness of a simple and flexible, DVR grid based approach for empirical improvement of molecular PESs. The method suggested does not rely on a predefined form of the correction surface and provides a

dx.doi.org/10.1021/jp504348f | J. Phys. Chem. A 2014, 118, 6256−6265

correction surface defined on the DVR grid points used. Refinement of the PES is based upon a minimization of an objective function utilizing selected experimental data along with other possible terms to force predefined properties on the correction surface, most importantly improving its "smoothness".

The algorithm was tested on the ground electronic state of the diatomic molecule MgH, for which an extremely accurate reference PES, obtained by Le Roy et al.,[7] is available. On the basis of the numerical results obtained, the following conclusions can be made concerning the empirical PES refinement procedure proposed:

(1) With the number of DVR grid points greatly exceeding the number of experimental energy levels included during the refinement procedure, additional terms must be included in the objective function to arrive at a physically meaningful, "smooth" correction surface. The optimal parametrization of these additional terms is not necessarily straightforward, as some values can lead to oscillations in the correction values, whereas others can cause unphysical "rigidity" in the surface. Numerical experience suggests that one should use λ_l values (eq 6) that ensure the damping of the correction surface to zero at coordinate regions where the wave functions included in the optimization do not have significant amplitudes, whereas μ and σ (see eq 7) should be set to very small values and gradually increased up to the point where the correction surface is "smooth enough" (oscillations becoming smaller than a few tenths of cm^{-1} was used as a criterion in this work). The "smoothness" could be monitored either by visual inspection of the correction surface or by evaluating the norm of eq 11.

(2) Using simple first-order perturbation theory (PT1) in the objective function to account for the presence of PES correction values seems to work very well, as for MgH it gives results almost identical to those for second-order PT, except for large (>4 Å) internuclear distances, where 1−2 cm^{-1} differences could be observed. The fact that only a minor part of a single wave function has nonzero amplitude in that coordinate region explains the observed behavior.

(3) For a given J rotational quantum number, the corrected PES is able to reproduce experimental (ro)vibrational eigenenergies to a few hundredths of a cm^{-1} if they are included during the optimization, and to within a few tenths of a cm^{-1} if they are interpolated; *i.e.*, they lie between two states (in energy) that are included during the optimization. Extrapolated states tend to have somewhat larger errors.

(4) The PES optimized on vibrational states results in a small, on the order of 0.1 cm^{-1}, and more or less systematic error for the rovibrational states.

(5) When the number of experimental values included during the optimization greatly exceeds the number of grid points upon which the PES is optimized, outstanding accuracy, with average errors on the order of 0.01 cm^{-1}, could be achieved for all vibrational and rotational quantum numbers (Table 3).

(6) Resonance energies and widths computed using the MLR PES of ref 7 can be reproduced with considerable accuracy using the refined PESs. Similarly to bound states, the inclusion of additional rovibrational states to the vibrational states during optimization leads to more accurate results.

(7) For a given v vibrational quantum number, inclusion of resonance states into the objective function can lead to significant wave function amplitudes at coordinate ranges where the bound states vanish; thus, they lead to an improved refined PES. However, in the case of MgH, if all the bound states (up to $J = 44$) are included into the objective function, the additional inclusion of the resonance states presented in Table 4 does not extend the coordinate range having significant wave function amplitudes.

(8) Application of the method presented to polyatomic molecules, although straightforward in principle, may need special considerations.

AUTHOR INFORMATION

Corresponding Author

*A. G. Császár: e-mail, csaszar@chem.elte.hu.

Notes

The authors declare no competing financial interest.

ACKNOWLEDGMENTS

The work described received support from the Hungarian Scientific Research Fund (OTKA NK83583), from an ERA-Chemistry grant, and from TÁMOP 4.2.4. A/1-11-1-2012-000 "National Excellence Program − Elaborating and operating an inland student and researcher personal support system", a project subsidized by the European Union and cofinanced by the European Social Fund. We owe special thanks to Professor Robert J. Le Roy, for his suggestion to study MgH and the valuable information he provided regarding MgH and the corresponding MLR PES.

REFERENCES

(1) Born, M.; Oppenheimer, J. R. Zur Quantentheorie der Molekeln. *Ann. Phys.* **1927**, *389*, 457−484.

(2) Jordan, M. J. T.; Thompson, K. C.; Collins, M. A. Convergence of molecular potential energy surfaces by interpolation: Application to the OH + H_2 → H_2O + H reaction. *J. Chem. Phys.* **1995**, *102*, 5647−5657.

(3) Manzhos, S.; Wang, X.; Dawes, R.; Carrington, T. A nested molecule-independent neural network approach for high-quality potential fits. *J. Phys. Chem. A* **2006**, *110*, 5295−5304.

(4) Pastrana, M. R.; Quintates, M. A. L.; Brandao, J.; Varandas, A. J. C. Recalibration of a single-valued double many-body expansion potential energy surface for ground-state hydroperoxy and dynamics calculations for the O + OH → O_2 + H reaction. *J. Phys. Chem.* **1990**, *94*, 8073−8080.

(5) Carter, S.; Culik, S. J.; Bowman, J. M. Vibrational self-consistent field method for many-mode systems: A new approach and application to the vibrations of CO adsorbed on Cu(100). *J. Chem. Phys.* **1997**, *107*, 10458−10469.

(6) Rauhut, G. Efficient calculation of potential energy surfaces for the generation of vibrational wave functions. *J. Chem. Phys.* **2004**, *121*, 9313−9322.

(7) Henderson, R. D. E.; Shayesteh, A.; Tao, J.; Haugen, C. C.; Bernath, P. F.; Le Roy, R. J. Accurate analytic potential and Born−Oppenheimer breakdown functions for MgH and MgD from a direct-potential-fit data analysis. *J. Phys. Chem. A* **2013**, *117*, 13373−13387.

(8) Császár, A. G. Anharmonic molecular force fields. *Wiley Interdiscip. Rev.: Comput. Mol. Sci.* **2012**, *2*, 273−289.

(9) Partridge, H.; Schwenke, D. W. The determination of an accurate isotope dependent potential energy surface for water from extensive *ab*

initio calculations and experimental data. *J. Chem. Phys.* **1997**, *106*, 4618−4639.
(10) Shirin, S. V.; Polyansky, O. L.; Zobov, N. F.; Ovsyannikov, R. I.; Császár, A. G.; Tennyson, J. Spectroscopically determined potential energy surfaces of the $H_2{}^{16}O$, $H_2{}^{17}O$, and $H_2{}^{18}O$ isotopologues of water. *J. Mol. Spectrosc.* **2006**, *236*, 216−223.
(11) Yachmenev, A.; Yurchenko, S. N.; Jensen, P.; Thiel, W. A new "spectroscopic" potential energy surface for formaldehyde in its ground electronic state. *J. Chem. Phys.* **2011**, *134*, 244307.
(12) Császár, A. G.; Fábri, C.; Szidarovszky, T.; Mátyus, E.; Furtenbacher, T.; Czakó, G. The fourth age of quantum chemistry: Molecules in motion. *Phys. Chem. Chem. Phys.* **2012**, *14*, 1085−1106.
(13) Tennyson, J.; Bernath, P. F.; Brown, L. R.; Campargue, A.; Császár, A. G.; Daumont, L.; Gamache, R. R.; Hodges, J. T.; Naumenko, O. V.; Polyansky, O. L.; Rothman, L. S.; Vandaele, A. C.; Zobov, N. F.; Al Derzi, A. R.; Fábri, C.; Fazliev, A. Z.; Furtenbacher, T.; Gordon, I. E.; Lodi, L.; Mizus, I. I. IUPAC Critical Evaluation of the Rotational-Vibrational Spectra of Water Vapor. Part III. Energy Levels and Transition Wavenumbers for $H_2{}^{16}O$. *J. Quantum Spectrosc. Radiat. Transf.* **2013**, *117*, 29−58.
(14) Tarczay, G.; Császár, A. G.; Klopper, W.; Quiney, H. M. Anatomy of relativistic energy corrections in light molecular systems. *Mol. Phys.* **2001**, *99*, 1769−1794.
(15) Pyykkö, P.; Dyall, K. G.; Császár, A. G.; Tarczay, G.; Polyansky, O. L.; Tennyson, J. Estimation of Lamb shifts effects for molecules. Application to the rotation-vibration spectra of water. *Phys. Rev. A* **2001**, *63*, 024502.
(16) Handy, N.C.; Yamaguchi, Y.; Schaefer, H. F., III. The diagonal correction to the Born−Oppenheimer approximation: Its effect on the singlet−triplet splitting of CH_2 and other molecular effects. *J. Chem. Phys.* **1986**, *84*, 4481−4484.
(17) Moss, R. E. On the adiabatic and nonadiabatic corrections in the ground electronic state of the hydrogen molecular cation. *Mol. Phys.* **1996**, *89*, 195−210.
(18) Furtenbacher, T.; Szidarovszky, T.; Mátyus, E.; Fábri, C.; Császár, A. G. Analysis of the rotational-vibrational states of the molecular ion H_3^+. *J. Chem. Theory Comput.* **2013**, *9*, 5471−5478.
(19) Pavanello, M.; Adamowicz, L.; Alijah, A.; Zobov, N. F.; Mizus, I. I.; Polyansky, O. L.; Tennyson, J.; Szidarovszky, T.; Császár, A. G.; Berg, M.; Petrignani, A.; Wolf, A. Precision measurements and computations of transition energies in rotationally cold triatomic hydrogen ions up to the midvisible spectral range. *Phys. Rev. Lett.* **2012**, *108*, 023002.
(20) Bunker, P. R.; Moss, R. E. The breakdown of the Born−Oppenheimer approximation: the effective vibration-rotation Hamiltonian for a diatomic molecule. *Mol. Phys.* **1977**, *33*, 417−424.
(21) Bunker, P. R.; Moss, R. E. The effect of the breakdown of the Born-Oppenheimer approximation on the rotation-vibration Hamiltonian of a triatomic molecule. *J. Mol. Spectrosc.* **1980**, *80*, 217−228.
(22) Diniz, L. G.; Mohallem, J. R.; Alijah, A.; Pavanello, M.; Adamowicz, L.; Polyansky, O. L.; Tennyson, J. Vibrationally and rotationally nonadiabatic calculations on H_3^+ using coordinate-dependent vibrational and rotational masses. *Phys. Rev. A* **2013**, *88*, 032506.
(23) Polyansky, O. L.; Tennyson, J. *Ab initio* calculation of the rotation−vibration energy levels of H_3^+ and its isotopomers to spectroscopic accuracy. *J. Chem. Phys.* **1999**, *110*, 5056−5064.
(24) Harris, D. O.; Engerholm, G. G.; Gwinn, W. D. Calculation of matrix elements for one-dimensional quantum-mechanical problems and the application to anharmonic oscillators. *J. Chem. Phys.* **1965**, *43*, 1515−1517.
(25) Dickinson, A. S.; Certain, P. R. Calculation of matrix elements for one-dimensional quantum-mechanical problems. *J. Chem. Phys.* **1968**, *49*, 4209−4211.
(26) Lill, J. V.; Parker, G. A.; Light, J. C. Discrete variable representations and sudden models in quantum scattering theory. *Chem. Phys. Lett.* **1982**, *89*, 483−489.
(27) Nikolaos, S. Finite Difference schemes on non-uniform meshes for hyperbolic conservation laws, *Doctoral thesis* (2009).
(28) Dennis, J. E.; Schnabel, R. B. *Numerical methods for unconstrained optimization and nonlinear equations*; Prentice-Hall: Englewood Cliffs, NJ, 1983.
(29) Shayesteh, A.; Henderson, R. D. E.; Le Roy, R. J.; Bernath, P. F. Ground state potential energy curve and dissociation energy of MgH. *J. Phys. Chem. A* **2007**, *111*, 12495−12505.
(30) Tennyson, J.; Sutcliffe, B. T. Variationally exact ro-vibrational levels of the floppy CH_2^+ molecule. *J. Mol. Spectrosc.* **1983**, *101*, 71−82.
(31) Moiseyev, N. *Non-Hermitian quantum mechanics*; Cambridge University Press: Cambridge, U.K., 2011.
(32) Poirier, B.; Carrington, T. Semiclassically optimized complex absorbing potentials of polynomial form. I. Pure imaginary case. *J. Chem. Phys.* **2003**, *118*, 17−28.
(33) Riss, U. V.; Meyer, H.-D. Calculation of resonance energies and widths using the complex absorbing potential method. *J. Phys. B: At. Mol. Opt. Phys.* **1993**, *26*, 4503−4536.
(34) Landau, L. D.; Lifshitz, E. M. *Quantum Mechanics*; Pergamon: Oxford, U.K., 1965.
(35) Kukulin, V. I.; Kasnopolsky, V. M.; Horacek, J. *Theory of resonances*; Kluwer: Dordrecht, The Netherlands, 1988.
(36) Le Roy, R. J.; Chapman, S. G.; McCourt, R. W. Accurate thermodynamic properties of the six isotopomers of diatomic hydrogen. *J. Phys. Chem.* **1990**, *94*, 923−929.
(37) Smith, F. T. Collision lifetimes and the thermodynamics of real gases. *J. Chem. Phys.* **1963**, *38*, 1304−1310.